RAP CONFERENCE PROCEEDINGS, VOL. 8, PP. 142–149, 2023
ISSN 2737-9973 (ONLINE) | DOI: 10.37392/RAPPROC.2023.29
RAP-PROCEEDINGS.ORG

# SPECTROSCOPIC ANALYSIS AND CHARGED PARTICLE IDENTIFICATIONS OF THERMAL AND FAST NEUTRON DOSIMETRY USING NUCLEAR TRACK DETECTORS (NTDS)

**E. H. Ghanim[1*], S. M. Othman[2], A. Hussein[2], H. El-Samman[2], A. El-Sersy[3]**

[1]Basic Sciences Department, Faculty of Technology and Education, Beni-Suef University, Beni-Suef, Egypt
[2]Physics Department, Faculty of Science, Menoufiya University, Shebin El-Koam, Egypt
[3]Ionizing Radiation Depart, National Institute for Standards (NIS), Tersa Street, El Haram Giza, Egypt

***Abstract.*** *In this work, nuclear track detectors (NTDs) of CR-39 and LR-115 were used in identification of charged particles and determination of doses of fast and thermal neutrons. CR-39 characterizations were carried out using etchant conditions of 6N NaOH at 60°C with $V_B \approx 0.9$ µm/hr with registration efficiency better than 90 % and critical angle of etching under different removal layer values. In addition, CR-39 NTDs were used in fast neutron registration utilizing their interactions with the constituent atoms of the detector material. Induced-proton track densities (ρT) were registered at different etching times and neutron doses (Dfn) from 1.54 up to ≈ 44 mSv. An exponential relationship between ρT and Dfn was found to obey the formula Dfn = 1.27 exp ( 0.067 ρT). An empirical formula to relate the induced proton energy ($E_p$) with its $(dE/dx)_p$ in CR-39 was found to be $E_p = 170.031\ (dE/dx)_p^{-1.518}$ MeV/µm. Also, in this work, CR-39 and LR-115 track detectors were used for detection of dose of thermal neutrons obtained through the polymethyle methacrylate sheet (PMMA) moderation of $^{241}$Am-Be fast neutrons source with $B_2O_3$ converter. CR-39 and LR-115 NTDs were exposed to thermal neutrons for up to 37 hrs. Four sets of detectors were irradiated at exposure times of 1.5, 18, 21 and 37 hrs. The thermal neutron fluxes were calculated from the induced-ions track density through the concepts of the efficiency factor from the total track density ($\rho_T$). The equivalent doses (D) of thermal neutrons were deduced using the dose-flux relationship or flux-dose conversion factor. Moreover, $^{7}$Li (0.84 MeV) and $^{4}_{2}$He (1.47 MeV) induced-ion tracks were produced from the interaction of thermal neutrons with boron-covered CR-39 detector. The discrimination between alpha panicles ($^{4}_{2}$He –ions) and $^{7}$Li-ions was carried out extensively. Data measurements were repeated many times in order to achieve better accuracy. This discrimination (or spectroscopic analysis) is based on an adequate and careful analysis of the acquired data obtained from the circular track diameters induced in CR-39 detectors as a result of thermal-neutron-boron interaction mechanisms. The charged particles ($^{4}$He, $^{7}$Li) identifications were successfully obtained using circular-track diameter analysis method with alpha tracks from $^{241}$Am alpha reference source. Although such method is tedious, results are indeed encouraging and certainly recommended. Results of this study are then discussed within the frame work of track formation theories and etching mechanism in NTDs.*

***Keywords:*** *CR-39, LR-115, NTDs, fast neutron, proton tracks, dE/dx, thermal neutron, induced-ions tracks ($^{7}$Li-$^{4}$He)*

## 1. INTRODUCTION

Nuclear track detectors (NTDs) are widely employed in many scientific studies and several technological applications [1-12]. Track detectors are successfully used in the determination of U and Th in natural samples, as personnel neutron dosimeters, in charged particle identification, radon survey studies, alpha-radio-autography, etc. [13-23]. They provide permanent records of events (tracks), operate successfully under various environmental conditions and have almost no fading under normal storage conditions. Each charged incident particle on the surface of a NTD interacts and leaves a trail of damaged material which can be read with an optical microscope after an etching process takes place. Studying the characterizations of etched tracks reflects the properties of the type of interactions between incident radiation and the detector material [24-27]. Alpha incident particles produce alpha tracks, while induced proton tracks result from neutron interaction after elastic scattering process.

The aim of this work concentrates on studying the experimental registrations of alpha and recoil proton tracks in NTDs in order to enhance the dosimetric properties of such NTDs and the possibility of using them as good fast and thermal neutron dosimeters in certain specified fields. Also, the interaction of thermal neutrons with boron covered CR-39 and LR-115 track detectors is the main task of this paper. Dosimetric properties of thermal neutron irradiated CR-39 NTDs are studied. The product-ions discrimination method is used with circular track diameter measurements to evaluate thermal neutron doses. Mono-energetic alphas from $^{241}$Am-source were also used as reference alpha tracks to ensure the validity of such distinguishability technique in spectroscopic analysis and dosimetric applications.

* emadhamed_65@yahoo.com

## 2. Experimental Techniques

### *2.1. Materials, Etchants and Track Counting*

Two different types of NTDs were used in this study:

(1) CR-39 NTDs of 500 μm thicknesses, TASTRAK, ($C_{12}H_{18}O_7$, ρ=1.3 gm/cm³), manufactured by Ltd Comp, Bristol, UK, and

(2) LR-115 type II NTDs of 12 μm thickness layer (density ρ=1.3 gm/cm³, $C_6H_8O_7N_2$), manufactured by Kodak Pâthé Company, France.

These NTDs were irradiated by alpha and neutron sources and then chemically etched before track measurements. Chemical Etchants of 6.0 N NaOH at 70°C and 2.5 N NaOH at 60°C were used with CR-39 and LR-115 NTDs, respectively. An optical microscope (Olympus BH-2) with eye piece lens of 0.22 μm per division and attached digital camera was used in track counting and track parameters measuring.

### *2.2. Irradiation Facilities*

CR-39 and LR-115 detectors were exposed to $^{241}$Am alpha source (0.924 μCi) and to $^{241}$Am-Be fast neutron source (5.0 Ci).

### *2.3. Thermal Neutron Detection*

Thermal neutrons were obtained from the moderation of $^{241}$Am-Be fast neutrons using sheets of equal thickness of polymethyle methacrylate (PMMA). It was found that 6 cm PMMA sheet is sufficient to thermalize about 95% of the fast neutron flux from $^{241}$Am-Be source. The thermal neutron doses were measured using CR-39 and LR-115 NTDs covered with $B_2O_3$ as a converter [4]. Samples of CR-39 were irradiated at different times up to 37 h by thermal neutrons from $^{241}$Am-Be source using boron oxide as a converter.

## 3. Results and Discussion

### *3.1. Alpha Particles Identifications*

#### *3.1.1. Registration Efficiency*

The alpha registration efficiencies of both CR-39 and LR-115 track detectors were determined as a function of alpha energy from 0.5 to 5.48 MeV. Efficiency is defined as the ratio of the number of track density per unit exposure time (ρ/t) to the number of the incident alpha particle flux ($\varphi$), given in alpha/cm².

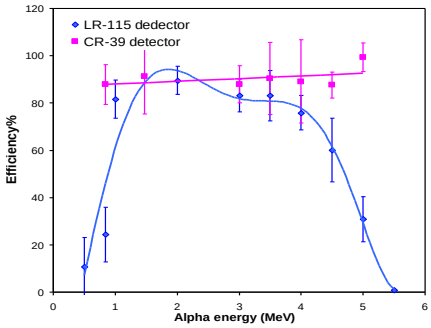


Figure 1. Comparison between registration efficiencies for CR-39 and LR -115 track detectors versus values of alpha energy.

Figure 1 shows the variation of efficiency (%) with alpha energy for both CR-39 and LR-115 track detectors. From Figure 1, one sees that the efficiency value of LR-115 is about 80% in energy range from 1.5 to 3.5 MeV and then decreases with increase in energy, while the efficiency of CR-39 is nearly 95 % in the entire studied energy range.

### *3.2. Fast Neutron Detection*

#### *3.2.1. Fast Neutron Dosimetry*

CR-39 foils were irradiated by $^{241}$Am-Be neutron source at different doses (1.451, 8.651, 23.581, and 44.005 mSv). Irradiated samples were chemically etched (6N NaOH at 60°C) for different etching durations, then the diameter of the induced proton tracks was measured under an optical microscope.

Figure 2 (a, b, c, and d) shows the variation of induced recoil proton track density with etching time. The track density shows a strong increase with etching time.

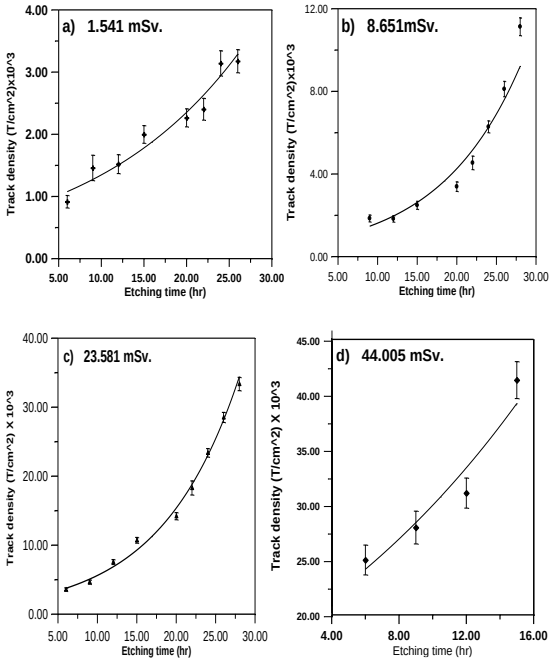


Figure 2. Track density as a function of etching time at different neutron doses in CR-39 NTDs.

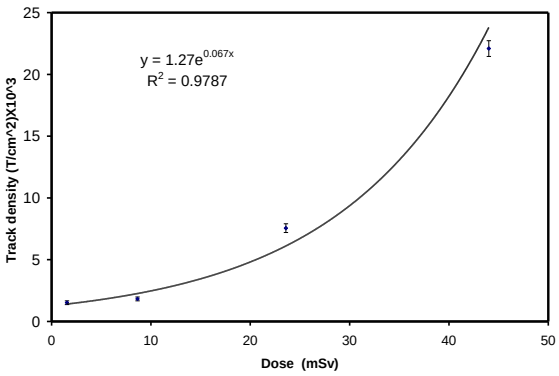


Figure 3. Track density as a function of fast neutron dose at value of removal layer of 10.9 μm.

Figure 3 shows a relationship between the track density and dose values. This figure provides a calibration curve which can be used in fast neutron dosimetry, for any future study, when one needs to evaluate the fast neutron-dose rate with track density measurements. In this case some plastic detectors etched under the same conditions should be used in the measurement. CR-39 was etched in 6N NaOH at 60°C and for 12 hr.

### *3.2.2. Fast Neutron Spectroscopy and Identification*

The fast neutron spectroscopy was carried out by the measurement of the neutron-induced proton tracks due to elastic scattering of fast neutrons with constituent atoms in CR-39 detector. The energy of the induced protons $E_p$ is governed by its scattering angle (θ) according to well-known equation [22]:

$$E_p = \frac{4A}{(A+1)^2}\cos^2\theta\, E_n \qquad (1)$$

where θ is the scattering angle of the proton and A is the target atomic mass.

In a special case when the scattering angle is zero, the proton energy is maximum and equals neutron energy, $E_p = E_n$. In NTDs the circular tracks mean that the scattering angle is zero and so the proton energy is equal to the neutron energy. This method is used in this work for neutron spectroscopy.

In this work, the recoil proton track diameters in CR-39 detector were used to study the distribution of the neutron energies from $^{241}$Am-Be source. The diameters of the circular tracks were measured under etchant conditions of 6 Na OH at 60°C.

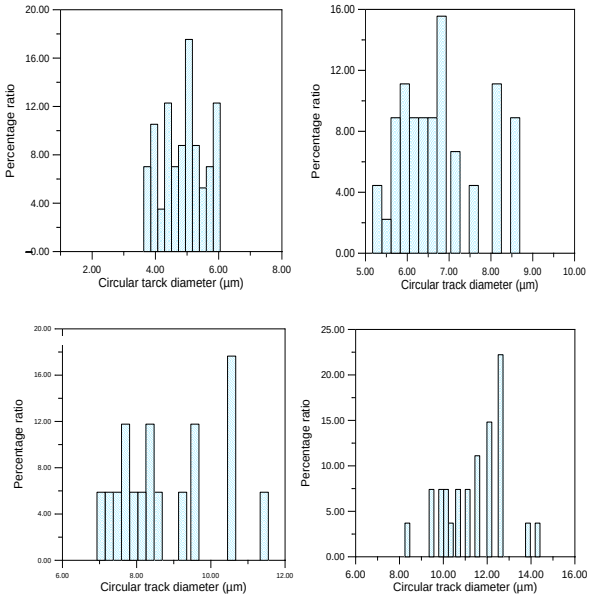


Figure 4. Histogram distribution of induced protons circular tracks in CR-39 irradiated by fast neutrons to a dose of 1.541 mSv at different removal layers.

The relation between the fractional percentage numbers of measured circular induced proton tracks with their corresponding diameters are shown in Figures 4-6. These measurements were performed at various removal layers and neutron doses (1.451, 8.651, and 44.005 mSv). At least a total of circular track was counted and considered in measurements. The neutron spectroscopy study can then be easily investigated by the aid of Figures 6-8, where the registered circular induced proton track distributions are taken into consideration.

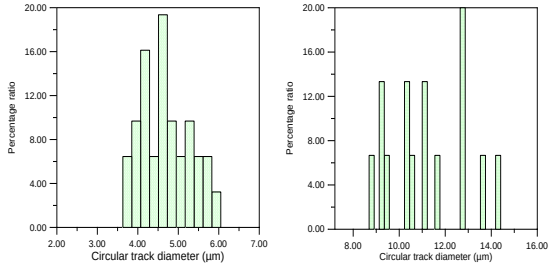


Figure 5. Distribution of induced protons circular tracks in CR- 39 irradiated by fast neutrons to a dose of 8.651 mSv at different removal layers.

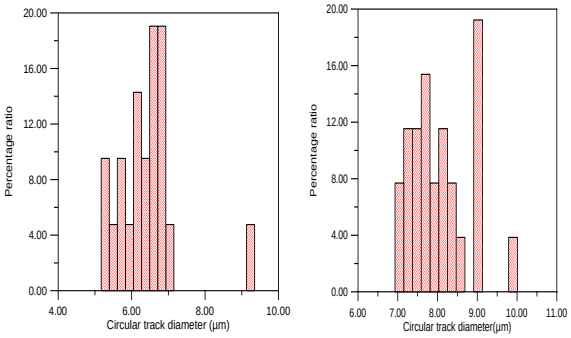


Figure 6. Distribution of induced protons circular tracks in CR-39 irradiated by fast neutrons to dose of 44 mSv at different removal layers.

Fast neutron spectroscopy of the Am-Be source can be established if one is able to relate the circular proton tracks (see Figures 4-6) to proton energies. This cannot be achieved without a monoenergetic proton-energy source. Instead of such requirement, a relation between the response function or velocity ratio V, and the function dE/dX (energy loss per unit path length of protons in CR-39 detector) can be used, (dE/dX-V) by Yamauchi et al; 1999 [27] as

$$[\,dE/dX\ (Kev/\mu m)]_p = 109.395 \log\,(V) - 3.375 \qquad (2)$$

where p stands for proton.

Figures 7-9 show the percentage ratio of circular proton tracks and the etching ratio V at various neutron doses. V is calculated from the formula [21]:

$$V=\frac{h^2+r^2}{h^2-r^2} \qquad (3)$$

where h hand r are the removal layer and the radius of the circular proton-track, respectively. It is clear from these figures that V ranges from 1.2 to about 1.8.

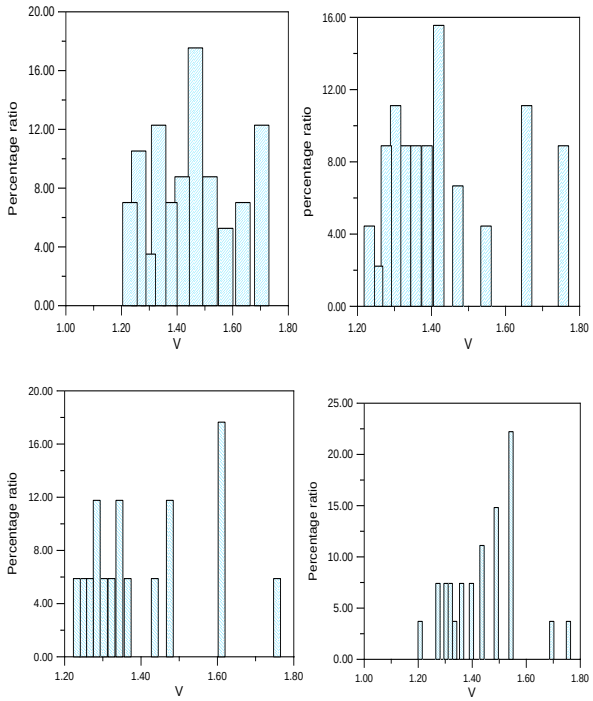


Figure 7. Distribution of the response function (V) of circular-proton tracks in CR-39 irradiated by fast neutrons to a dose 1.541 mSv and different removal layers.

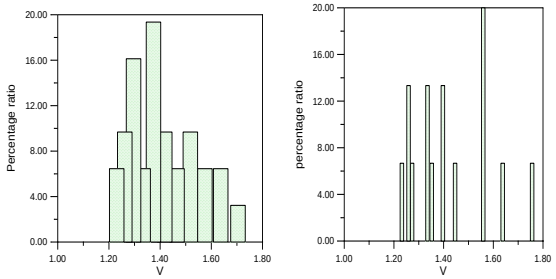


Figure 8. Distribution of the response function (V) of circular-proton tracks in CR-39 irradiated by fast neutrons to a dose of 8.651 mSv and different removal layers.

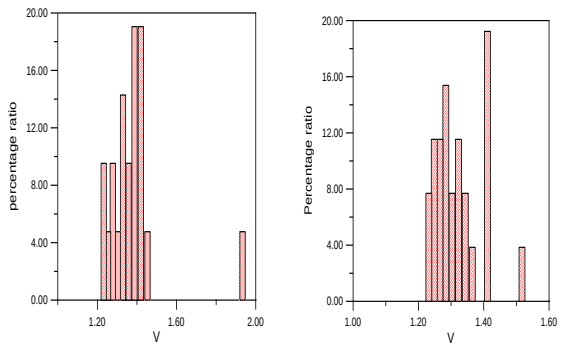


Figure 9. Distribution of the response function (V) of circular- proton tracks in CR-39 irradiated by fast neutrons to a dose of 44 mSv and different removal layers.

Using the relation (3), one can obtain representation given in Figure 10 between V and proton $(dE/dX)_p$. Different models were done by many authors to get a factor between the energy loss $(dE/dX)_P$ of protons and the etch rate ratio V of the protons in CR-39; one of these models [1] is used, where [(dE/dX) - V] factor can be obtained.

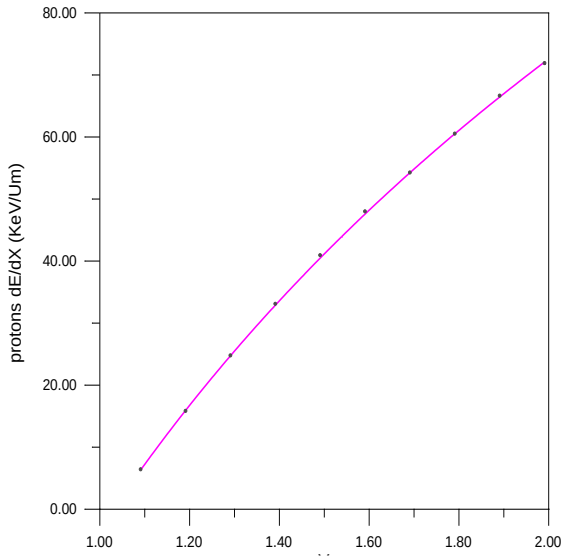


Figure 10. Proton energy loss rates (dE/dX) in CR-39 as a function of response function V.

By using SRIM-computer code program [3], one can extract a relationship between proton energy $E_P$ and $(dE/dX)_p$ in CR-39 detector which is given in Figure 11. A fitting formula can be represented in the form:

$$E_P = 170.031\ (dE/dx)_p^{-1.518} \qquad (4)$$

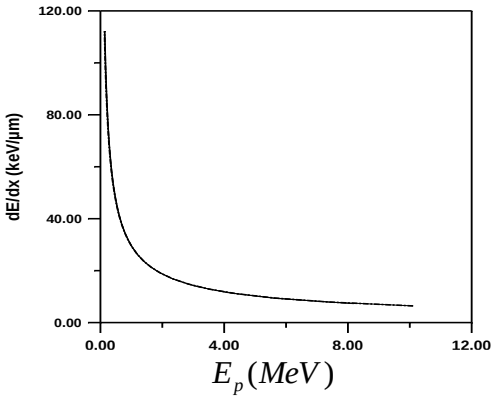


Figure 11. Rate of Energy loss; (dE/dX) calculated by SRIM computer program as a function of proton energy.

From the relationships (dE/dx vs V) and (dE/dx vs $E_P$) one can extract the dependence of V on $E_P$. Furthermore, since the track diameters are related to V, one can then relate track diameters to proton energies. Under the conditions of our treatment, the proton energies are supposed to be exactly the same as the energies of fast neutrons emitted from the $^{241}$Am-Be source. The representations given in Figures 4 to 6 can be transformed into energy representations instead of track diameters.

### *3.3. Thermal Neutron Detection*

#### *3.3.1. Thermal Neutron Dosimetry*

When thermal neutron is incident upon the layer of $^{10}$B, used as a converter, the reaction products, alpha particles ($^4$He) and $^7$Li-ions, emerge from Boron with energies of 1.47 and 0.54 MeV, respectively [5, 6]. The

ions hit the surface of the CR-39 detector with the same energy if they emerge just at the detector surface. Figure 12 shows the variation of alpha and Li track density with etching time at different exposure times. It is also convenient to use LR-115 detector in thermal neutron dosimetry because the induced alpha has energy within the registration energy window of LR-115.

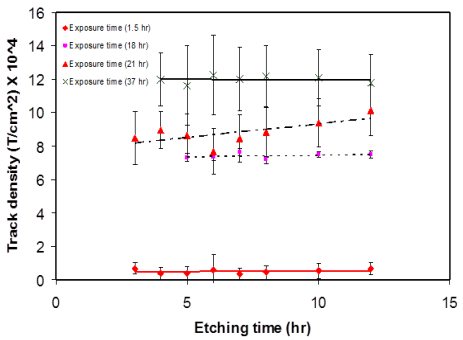


Figure 12. Track density registered in CR-39 using $B_2O_3$ converter versus etching time for thermal neutrons at different exposure times.

Figure 13 displays the variation of track densities registered in CR-39 and LR-115 using $B_2O_3$ converter versus thermal neutron exposure time. It is found (see Figure 13) that the density of tracks registered in CR-39 is higher than that registered in LR-115. This is most probably attributed to the higher registration efficiency of CR-39 than that of LR-115.

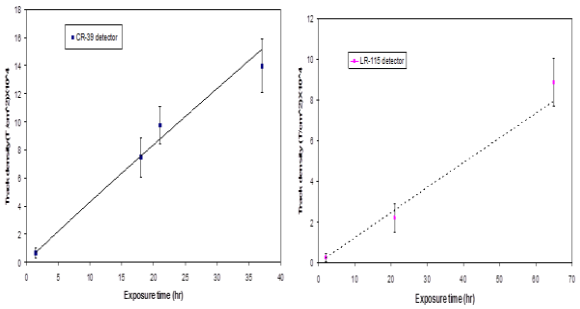


Figure 13. Track densities registered in CR-39 and LR-115 using $B_2O_3$ converter as a function of thermal neutron exposure time.

### *3.3.2. Thermal neutron dose determination*

CR-39 and LR-115 track detectors were used for thermal neutron dose measurements using $B_2O_3$ as a converter. For thermal neutron dose determination using CR-39 and LR-115 detectors, the thermal neutron flux should be obtained from the induced-ions track density. The fluence is obtained by means of the efficiency factor as follows.

The total efficiency $\eta$ is given by:

$$\eta = \varepsilon X \qquad (5)$$

where $\varepsilon$ is the registration efficiency and X is etching efficiency of induced alpha particles and is given by:

$$X = \frac{1}{4} R\cos^2\theta_c \qquad (6)$$

where R is the range of 1.47 MeV alpha particle in $B_2O_3$ and $\theta_c$ is the critical angle of etching. The thermal neutron flux $\emptyset$ can be obtained from the total track density $\rho$ as [21]:

$$\rho = \eta \emptyset t \qquad (7)$$

From the flux calculation, one can calculate the equivalent dose (D) from the dose-flux conversion relationship factor, which is given by:

$$D = H\Phi \qquad (8)$$

where H is the flux-dose converting factor [28], which has a value of $1.07X\ 10^{-15}$ Sv·m$^2$.

Figure 14 shows the thermal neutron dose in CR-39 and LR-115 using B2O3 converter versus exposure time for thermal neutrons.

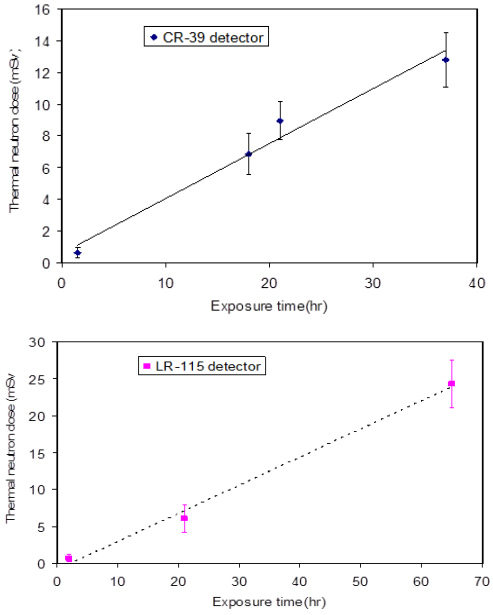


Figure 14. Thermal neutron dose in CR-39 and LR-115 using $B_2O_3$ converter versus exposure time.

### *3.3.3. Thermal Neutron-Induced-Charged Particle Identification (He, Li)*

When thermal neutrons irradiate boron-covered CR-39 detector, resulting particles $^7$Li (0.84 MeV) and $^4_2$He (1.47 MeV) induce tracks. Ranges of $^7$Li ions are lower than those of $^4_2$He ions. The discrimination between alpha particles and Li ions was extensively carried out and data measurements were repeated many times in order to achieve better accuracy in measurements. This discrimination (or spectroscopy analysis) is based on an adequate and careful analysis of the acquired data obtained from the circular track diameters induced in CR-39 detectors as a result of thermal neutron-boron interaction mechanisms. This is a rather tedious task but good acceptable result should indeed be expected. Four sets of detectors were used, where each set was irradiated at different thermal neutron exposures. Times of exposure were 1.5, 18, 21 and 37 hrs.

Figure 15 (a & b) shows the variation of the numbers of circular tracks percent with their diameters registered in boron-covered CR-39 detectors exposed to 1.5 hr thermal neutrons. Two periods of etching time were used which correspond to removal layers of 6.4 and 7.3 μm. Etching conditions of 6N NaOH at 60°C

were used in all experiments. From inspection of data analysis/fitting curves one can have the following observations:

1- As a result from data-fitting method, two peaks were found (good energy discrimination) at each value or removal layer thickness. The first peak (lies on the left) corresponds to the Li-induced tracks, while peak to the right (second peak) corresponds to alpha particle-induced tracks. Peaks at longer etching time are shifted to the right, where diameters are increased. Results are expected and confirm the nature of track properties in matter.

2-The density of induced alpha tracks is larger than that of Li tracks. This may be due to smaller ranges of Li ions in comparison to alphas.

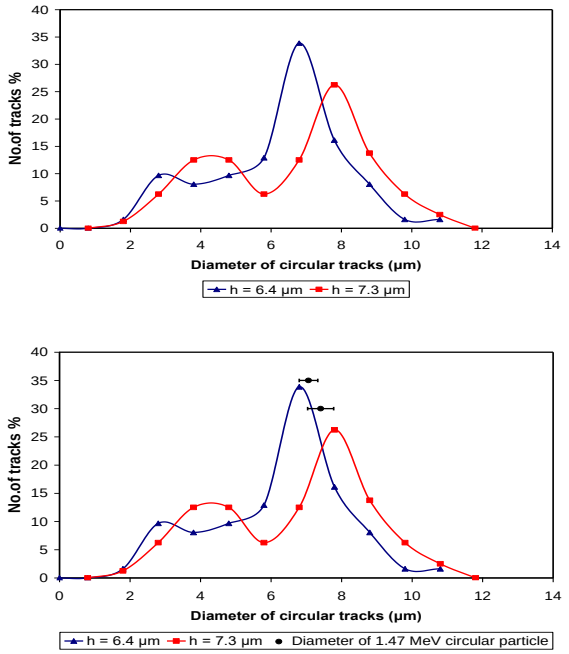


Figure 15. Distribution of circular tracks in CR-39 exposed to 1.5 hr thermal neutrons at different removal layers; (a) without reference tracks from $^{241}$Am-source and (b) with reference tracks.

In fact, we proceeded further to have a great confidence about such results by doing an additional experimental test using a standard alpha emitter ($^{241}$Am source) at a monoenergetic value of 1.47 MeV. For such case, additional CR-39 detectors were exposed to 1.47 MeV alphas, etched under the same etching conditions and tracks were measured at removal layers of 6.4 and 7.3 μm. Figure 15-b is the same as that given in Figure 15-a but with 1.47 MeV alpha tracks included using $^{241}$Am-source as reference points. It is clear from Figure 15-b that values of reference alpha tracks are consistent with the alpha-peak position within the experimental error uncertainty.

Figures 16-18 display the same detailed studies as in Figure 15-b, but with thermal neutron-exposure times of 18, 21 and 37 hrs, respectively. All measurements given in these figures were carried out at different removal thickness layers and the data were analyzed as explained in connection with Figure 15-b. In all figures reference alpha track-diameter representations were also included and an agreement with alpha peak-positions (within experimental error bars) was found.

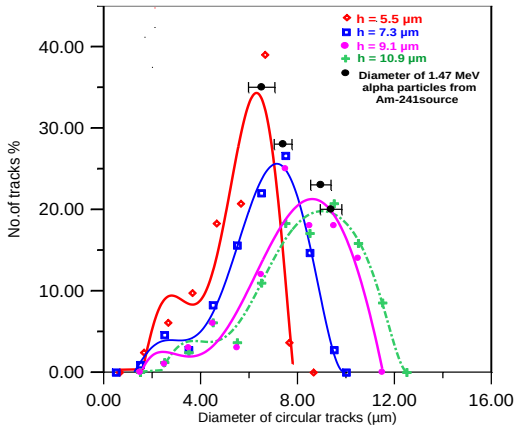


Figure 16. Distribution of circular tracks in CR- 39 exposed to 18 hr thermal neutrons at different removal layers.

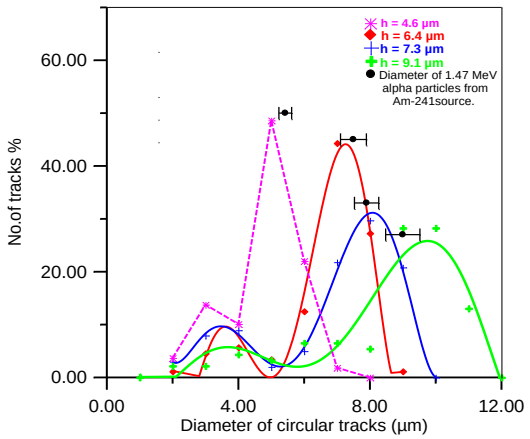


Figure 17. Distribution of circular tracks in CR-39 exposed to 21 hr thermal neutrons at different removal layers.

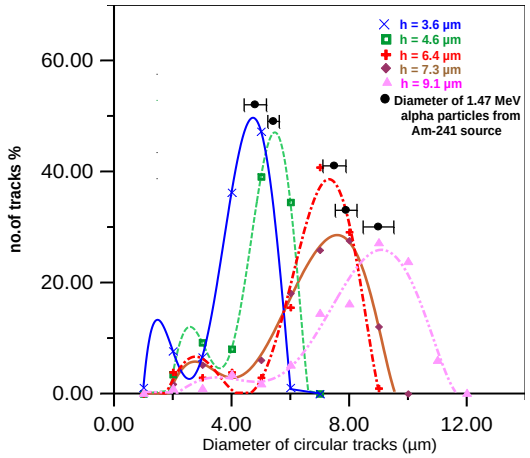


Figure 18. Distribution of circular tracks in CR- 39 exposed to 37 hr thermal neutrons at different removal layers.

The agreement between reference alpha tracks with alpha peak position at various removal layers strengthen the validity of presented data analyses and approximately determines the alpha-peak position as well as the Li-peak position in all measurements. As a closing remark, it can be said with confidence that alpha particles and Li-ions resulting from thermal neutron interaction with boron-covered CR-39 detector can be successfully discriminated using a simple method.

## 4. Conclusion

Nuclear track detectors (NTDs) have many advantages and are being used in various fields of science and technology.

Two types of track detectors were used in this study and various experiments were carried out to achieve the aim of the present work. The conclusion of the work can be summarized as follows:

1. Etching conditions of 6N and 2.5 N NaOH at 60°C were suitably used with CR-39 and LR-115 track detectors, respectively.

2. Detection efficiency of CR-39 for alpha track registration is better than 95% within the energy range of about 0.5 up to 5.5 MeV. The LR-115 showed a lower efficiency value of about 80% in the energy range 1.5 to 4.0 MeV; outside this latter energy window, the efficiency of LR-115 drops rapidly.

3. The fast neutron-induced proton track density in CR-39 showed a remarkable increase with increasing etching time and fast neutron dose. This reflects the importance and potential use of CR-39 detector in fast neutron dosimetry.

4. The use of CR-39 detector in fast neutron spectroscopy and neutron-induced recoil protons identifications can be carried out under fast neutron dose determination and selected value of removal layer thickness of CR-39 NTDs. Also, spectroscopic analysis of recoil tracks and fast neutron dose determination by using CR-39 detectors support the widespread applicability of NTDs in fast neutron dosimetric applications.

5. Fast neutron spectroscopy was well established by relating the neutron-induced proton track diameter (φ) to the etching rate ratio (V) and from (V-dE/dx) relationship, one can relate φ to dE/dx and then to proton or neutron energy as follows:

$$[\mathrm{dE/dx\ (Kev/\mu m)}]_p = 109.395 \log\ (\mathrm{V}) - 3.375$$

and

$$\mathrm{E_p} = 170.031\ (\mathrm{dE/dx})_p^{-1.518}$$

6. Fast neutron energy distribution was extended up to 10 MeV and it is in reasonable agreement with the energy distribution recorded from $^{241}$Am-Be neutron source.

7. The thermal neutron-induced-particle track density in CR-39 showed a remarkable increase with increasing etching time and thermal neutron dose. This reflects the importance and potential use of CR-39 detector in thermal neutron dosimetry.

8. The use of CR-39 detector in thermal neutron spectroscopy and neutron-induced charged particle identifications can be carried out under thermal neutron dose determination and selected value of removal layer thickness of CR-39 NTDs.

9. $^{6}$Li and $^{4}$He ions resulting from the interaction of thermal neutrons with boron-covered CR·39 are well resolved using the circular track diameter distribution method and checked with a monoenergetic alphas from $^{241}$Am-source.

10. Also, spectroscopic analysis of charged particle tracks and thermal neutron doses determination by CR-39 detectors support the widespread applicability of NTDs in thermal neutron dosimetric and particle identification applications.

11. Finally, it is recommended to use the suggested circular track diameter method used with PMMA to thermalize fast neutrons and applied spectroscopic analysis to other kinds of neutron sources in addition to $^{241}$Am-Be (i.e. Rd-Be, Ce-Be, etc.) in order to perform the thermal neutron dose measurements and charged particle identifications.

12. Finally, it is recommended to use the suggested circular track diameter method in fast and thermal neutron spectroscopic analysis to other kinds of neutron sources with CR-39, LR-115 and other NTDs.

## References


1. A. Al-Sayed et al., "Alpha particle spectrometry based on the mean grey level and visibility of track etch-pit in CR-39 Nuclear Track Detector," *Phys. Scr.*, vol. 97, no. 5, 055305, Apr. 2022. DOI: 10.1088/1402-4896/ac64d0
2. H. I. El-Naggar, E. H. Ghanim, M. El Ghazaly, T. T. Salama, "On the registration of low energy alpha particle with modified GafChromic EBT2 radiochromic film," *Radiat. Phys. Chem.*, vol. 191, 109852, Feb. 2022. DOI: 10.1016/j.radphyschem.2021.109852
3. E. H. Ghanim, M. El Ghazaly, H. I. El-Naggar, "Alpha particle detection by Makrofol DE1-1 and CR-39 NTDs: A comparative study," *Radiat. Phys. Chem.*, vol. 174, 108902, Sep. 2020. DOI: 10.1016/j.radphyschem.2020.108902
4. I. A. El-Mesady, Y. S. Rammah, A. M. Abdallah, E. H. Ghanim, "Gamma irradiation effect towards photoluminescence and optical properties of Makrofol DE 6-2," *Radiat. Phys. Chem.*, vol. 168, 108578, Mar. 2020. DOI: 10.1016/j.radphyschem.2019.108578
5. S. L. Guo, B. L. Chen, S. A. Durrani, "Solid-State Nuclear Track Detectors," in *Handbook of Radioactivity Analysis*, vol. 1, M. F. L'Annunziata, Eds., 4th ed., Cambridge (MA), USA: Academic Press, 2020, ch. 3, pp. 307 – 407. DOI: 10.1016/B978-0-12-814397-1.00003-0
6. T. S. Soliman, Sh. I. Elkalashy, M. F. Zaki, D. H. Shabaan, "Structural and optical analysis of gamma-induced modification in polycarbonate nuclear track detector," *Phys. Scr.*, vol. 96, no. 12, 125814, Sep. 2021. DOI: 10.1088/1402-4896/ac227d
7. V. Kumar, R. G. Sonkawade, A. S. Dhaliwal, "Gamma irradiation induced chemical and structural modifications in PM-355 polymeric nuclear track detector film," *Nucl. Instrum. Methods Phys. Res. B*, vol. 290, pp. 59 – 63, Nov. 2012. DOI: 10.1016/j.nimb.2012.08.029
8. Y. S. Rammah, A. M. Abdalla, "Study of the optical properties and the carbonaceous clusters in DAM-ADC solid state nuclear track detectors," *Radiat. Phys. Chem.*, vol. 141, pp. 125 – 130, Dec. 2017. DOI: 10.1016/j.radphyschem.2017.06.016
9. M. F. Zaki, "Gamma-induced modification on optical band gap of CR-39 SSNTD," *J. Phys. D Appl. Phys.*, vol. 41, no. 17, 175404, Aug. 2008. DOI: 10.1088/0022-3727/41/17/175404
10. Y. S. Rammah, S. E. Ibrahim, E. M. Awad, "Electrical and optical properties of Makrofol DE 1-1 polymeric films induced by gamma irradiation," *Bull. Natl. Res. Cent.*, vol. 43, 32, Feb. 2019. DOI: 10.1186/s42269-019-0071-4
11. D. Dobrev, J. Vetter, N. Angert, "Electrochemical preparation of metal microstructures on large areas of etched ion track membranes," *Nucl. Instrum. Methods Phys. Res. B*, vol. 149, no. 1 – 2, pp. 207 – 212, Jan. 2019. DOI: 10.1016/S0168-583X(98)00618-1

12. S. K. Chakarvarti, J. Vetter, "Template Synthesis-A membrane Based Technology for Generation of Nano-/Micro Materials," *Radiat. Meas.*, vol. 29, no. 2, pp. 149 – 159, Apr. 1998.
DOI: 10.1016/S1350-4487(98)00009-2
13. G. Szeiler et al., "Preliminary results from an indoor radon thoron survey in Hungary," *Radiat. Prot. Dosim.*, vol. 152, no. 1 – 3, pp. 243 – 246, Nov. 2012.
DOI: 10.1093/rpd/ncs231
14. S. A. Durrani, R. llic, *Radon Measurements by Etched track Detectors*, Hackensack (NJ), USA: World Scientific, 1997.
15. A. Hussein, "Determination of Uranium and Thorium Concentration in Some Egyptian Rock Samples," *J. Radioanal. Nucl. Chem.*, vol. 188, no. 4, pp. 255 – 265, Nov. 1994.
DOI: 10.1007/bf02164886
16. N. E. Khaled, E. H. Ghanim, Kh. Shinashin, A. R. El-Sersy, "Effect of X-ray energies on induced photo-neutron doses," *Radiat. Eff. Def. Solids*, vol. 169, no. 3, pp. 239 – 248, Mar. 2014.
DOI: 10.1080/10420150.2013.849250
17. G. W. Phillips et al., "Neutron spectrometry using CR-39 track etch detectors," *Radiat. Prot. Dosim.*, vol. 120, no. 1 – 4, pp. 457 – 460, Jan. 2006.
DOI: 10.1093/rpd/nci675
18. F. Castillo et al., "Fast neutron dosimetry using CR-39 track detectors with polyethylene as radiator," *Radiat. Meas.*, vol. 50, pp. 71 – 73, Mar. 2013.
DOI: 10.1016/j.radmeas.2012.09.007
19. A. R. El-Sersy, S. A. Eman, "Fast-Neutron Spectroscopy Studies using Induced-Proton Tracks in PADC Detectors," *Eur. Phys. J. A*, vol. 44, no. 3, pp. 397 – 401, Jun. 2010.
DOI: 10.1140/epja/i2010-10975-1
20. A. R. EI-Sersy, N. E. Khaled, S. A. Eman, "Thermal neutron dose determination with source geometry included," *Egypt. J. Biophys.*, B 12, pp. 131 – 142, 2006.
21. R. L. Fleischer, P. B. Price, R. M. Walker, *Nuclear Tracks in Solids: Principles and application*, Berkeley (CA), USA: University of California press, 1975.
DOI: 10.1525/9780520320239
22. S. A. Durrani, R. K. Bull, *Solid State Nuclear Track Detection. Principles, Methods and Applications*, 1st ed., Oxford, UK: Pergamon Press, 1987.
23. G. F. Knoll, *Radiation Detection and Measurement*, New York (NY), USA: J. Wiley and Sons, 1979.
24. K. R. Kase, W. R. Nelson, *Concepts of Radiation Dosimetry*, New York (NY), USA: Pergamon Press, 1978.
25. J. F. Ziegler, J. Bierack, "SRIM-The Stopping and Range of Ions in Matter," in *Treatise on Heavy-Ion Science*, vol. 6, D. A. Bromley, Eds., 1st ed., New York (NY), USA: Pergamon Press, 1985, ch. 3, pp. 93 – 129.
DOI: 10.1007/978-1-4615-8103-1_3
26. J. F. Ziegler, *SRIM-The Stopping and Range of Ions in Matter*, IBM Res., New York (NY), USA, 1996.
27. J. F. Ziegler, "SRIM-2003," *Nucl. Instrum. Methods Phys. Res. B*, vol. 219 – 220, pp. 1027 – 1036, Jun. 2004.
DOI: 10.1016/j.nimb.2004.01.208
28. T. Yamauchi, T. Taniguchi, K. Ода, "Study of Response of CR-39 Detector to Light Ions," *Radiat. Meas.*, vol. 31, no. 1 – 6, pp. 261 – 264, Jun. 1999.
DOI: 10.1016/S1350-4487(99)00127-4